Nucleon Energy Levels in a Diffuse Potential*

A. A. Ross,† Hans Mark, and R. D. Lawson
Department of Physics, University of California, Berkeley, California
(Received February 20, 1956)

The level sequence and shell structure for the bound single-particle states of nucleons moving in the spherically symmetric potential $V(r) = -V_0/[1+\exp\alpha(r-a)]$ have been examined. For protons, a Coulomb potential was added corresponding to a uniform charge distribution out to the "nuclear radius," a, and the potential depth was increased to give sufficient binding energy for the last proton level in the nucleus under consideration. For $\alpha = 1.45 \times 10^{+13}$ cm^{-1} (implying a surface layer of approximately 3×10^{-13} cm, which is constant for all A), a spin-orbit coupling 39.5 times the Thomas term and $a = 1.3 A^{\frac{1}{3}} \times 10^{-13}$ cm, good shell structure is obtained for both neutrons and protons. The level sequences obtained are in close agreement with experiment except in the region of strong distortion from sphericity. For $V_0 = 42.8$ Mev the neutron binding energies are in reasonable agreement with experiment. With these parameters the $3s$ and $4s$ giant resonances in the low-energy neutron scattering cross section occur at $A = 56$ and 166 respectively. The neutron and proton distributions in $_{79}$Au^{197} are examined. With the values of α, r_0, and λ given above, the thickness of the surface layer on the proton distribution is 1.92×10^{-13} cm and the radius is 6.77×10^{-13} cm.

INTRODUCTION

THE nuclear shell model,[1] which is based on the assumption that nucleons move independently in some average potential and experience a strong spin-orbit interaction, has had great success in predicting many of the ground-state properties of nuclei. It has generally been assumed that the collective nuclear potential is either a square well or an infinite harmonic oscillator, since for these potentials the wave equation is readily solvable. However, it is well known that neither a harmonic oscillator nor a finite square-well potential yields a satisfactory structure and sequence of bound-state neutron levels for the shell model. The harmonic oscillator, with spin-orbit coupling, is in fact only useful up to the twenty-nucleon shell. Thereafter the higher angular momentum states are too lightly bound and there is not even a shell at twenty-eight nucleons. The heavier nuclei are better represented by a finite square well with spin-orbit coupling, but, in contrast to the harmonic oscillator, the states of high angular momentum lie too low. It is possible to obtain shells everywhere except at 126, although the level sequence is far from satisfactory. At 126, the $1i_{11/2}$ level still lies below the $3p_{1/2}$ level even with a spin-orbit coupling forty times as large as the Thomas term. Also at 82 neutrons the shell is a little indefinite because the $1h_{9/2}$ level lies too low. The shell structure cannot be improved by increasing the spin-orbit coupling because for larger values the level with $j = l - \frac{1}{2}$ is shifted less than the level with $j = l + \frac{1}{2}$ since the lower level has a wave function with a larger value at the surface of the nucleus. For example, the $1i_{13/2}$ level would encroach on the 82 shell before the $1i_{11/2}$ level is raised enough to create a shell at 126.

It has been pointed out by several authors[2] that the true level sequence for the shell model should lie somewhere between that of the harmonic oscillator and the square well; i.e., a diffuse well might give reasonable results. The structure and sequence of levels depends on the size of the surface region. The aim of this investigation is to find a diffuse potential and a magnitude for the spin-orbit coupling which is in good agreement with the experimentally determined nucleon level sequence.

Recently Green and Lee[3] have investigated an approximate solution of the potential $V = -V_0$ for $r \leqslant a$, $V = -V_0 \exp(a-r)/\delta a$ for $r \geqslant a$ in an effort to determine a potential with an improved level sequence. However, their analysis was carried out neglecting spin-orbit coupling so that definite conclusions about nuclear shell structure could not be drawn. Green[4] has pointed out that in order to obtain the general trend of binding energies it must be assumed that δ decreases with increasing A (mass number). The fact that the "nuclear radius," a, is proportional to $A^{\frac{1}{3}}$ would indicate that the thickness of the surface layer of the potential should be approximately constant, in agreement with the recent analysis carried out by the Stanford group.[5] Although only the proton charge distribution has been investigated experimentally, it can be shown by WKB approximation that a constant surface layer for the nucleon distribution implies a constant surface layer for the potential. The surface layer, Δ, is defined as the distance from the point where the potential (or nucleon distribution) has 90% of its maximum value to the point where it has 10%.

[1] M. G. Mayer, Phys. Rev. **75**, 1969 (1949); Haxel, Jensen, and Suess, Phys. Rev. **75**, 1766 (1949).

[2] See for example, M. G. Mayer and J. H. D. Jensen, *Elementary Theory of Nuclear Shell Structure* (John Wiley and Sons, Inc., New York, 1955); W. Heisenberg, *Die Physik der Atomkerne* (Friedrich Vieweg und Sohn, Braunschweig, 1949).
[3] Alex E. S. Green and Kiuck Lee, Phys. Rev. **99**, 772 (1955).
[4] Alex E. S. Green, Phys. Rev. **99**, 1410 (1955).
[5] Hahn, Ravenhall, and Hofstadter, Phys. Rev. **101**, 1131 (1956).

In the present work the bound states of the potential[6] $V=-V_0/[1+\exp\alpha(r-a)]$ have been studied. If α is chosen to be constant, then the surface layer is independent of A, in agreement with the electron scattering experiments. Further, since the nuclear radius is roughly proportional to $A^{\frac{1}{3}}$, we choose $a=r_0A^{\frac{1}{3}}$,

$$-\frac{\hbar^2}{2m}\frac{1}{r^2}\frac{d}{dr}\left(r^2\frac{dR}{dr}\right)+\left(-\frac{V_{0n}}{1+\exp[\alpha(r-a)]}+\frac{\hbar^2}{2m}\frac{l(l+1)}{r^2}-\frac{\lambda\hbar^2}{4m^2c^2}\frac{\alpha V_{0n}\exp[\alpha(r-a)]}{\{1+\exp[\alpha(r-a)]\}^2r}\left\{\begin{matrix}l\\-(l+1)\end{matrix}\right\}\right)R=ER,\quad(1)$$

where l is the orbital angular momentum of the particle. V_{0n} is the neutron well depth, λ is the spin-orbit coupling constant, and the operator $\boldsymbol{\sigma}\cdot\mathbf{l}$ in the spin-orbit coupling has been replaced by l and $-(l+1)$, its eigenvalues when operating on a state with $j=l+\frac{1}{2}$ and $j=l-\frac{1}{2}$, respectively.

On the other hand, a proton in the nucleus moves not only in the specifically nuclear potential, but also

where r_0 is a constant. It is well known that in order to get nuclear shell structure a strong spin-orbit interaction is needed; this is taken to be the usual Thomas term[7] multiplied by an appropriate constant. Therefore, in dealing with neutrons the radial Schrödinger equation which must be solved is

experiences a strong Coulomb repulsion. For simplicity it has been assumed that this repulsion is derivable from a uniform charge distribution which extends to the nuclear radius, a. Thus for a nucleus with Z protons, the Coulomb repulsion exerted on a proton is derived from the potential $[(Z-1)/2a]e^2[3-(r/a)^2]$ for $r\leqslant a$ and $[(Z-1)/r]e^2$ for $r\geqslant a$. Therefore, for protons the radial wave equation to be solved is

$$-\frac{\hbar^2}{2m}\frac{1}{r^2}\frac{d}{dr}\left(r^2\frac{dR}{dr}\right)+\left(-\frac{V_{0p}}{1+\exp[\alpha(r-a)]}+\frac{\hbar^2}{2m}\frac{l(l+1)}{r^2}\right.$$

$$\left.-\frac{\lambda\hbar^2}{4m^2c^2}\frac{\alpha V_{0p}\exp[\alpha(r-a)]}{\{1+\exp[\alpha(r-a)]\}^2r}\left\{\begin{matrix}l\\-(l+1)\end{matrix}\right\}+\frac{Z-1}{2a}e^2\left[3-\left(\frac{r}{a}\right)^2\right]\right)R=ER$$

$$\text{for } r\leqslant a,$$

$$-\frac{\hbar^2}{2m}\frac{1}{r^2}\frac{d}{dr}\left(r^2\frac{dR}{dr}\right)+\left(-\frac{V_{0p}}{1+\exp\alpha(r-a)}+\frac{\hbar^2}{2m}\frac{l(l+1)}{r^2}\right.$$

$$\left.-\frac{\lambda\hbar^2}{4m^2c^2}\frac{\alpha V_{0p}\exp[\alpha(r-a)]}{\{1+\exp[\alpha(r-a)]\}^2r}\left\{\begin{matrix}l\\-(l+1)\end{matrix}\right\}+\frac{Z-1}{r}e^2\right)R=ER\quad(2)$$

$$\text{for } r\geqslant a,$$

where V_{0p} is the proton well depth. The spin-orbit coupling parameter, λ, is assumed the same for neutrons and protons.

Although in an actual nucleus there are fewer protons than neutrons, the Coulomb energy is so large that the proton potential must be assumed to be stronger than the neutron potential in order to avoid a large neutron excess. For neutrons a value of V_{0n} can be chosen which gives reasonable agreement with the experimental binding energies in the region $A=90$ to 208. However, for protons, V_{0p} must be adjusted for each nucleus studied in order to give the observed (γ,p) threshold.

[6] This potential has been used by various authors: R. D. Woods and D. S. Saxon, Phys. Rev. **95**, 577 (1954); R. M. Sternheimer, Phys. Rev. **97**, 1314 (1955); Yennie, Ravenhall, and Wilson, Phys. Rev. **95**, 500 (1954); D. G. Ravenhall and D. R. Yennie, Phys. Rev. **98**, 277 (1955); Hahn, Ravenhall, and Hofstadter, reference 5.

[7] L. H. Thomas, Nature **117**, 514 (1926); D. R. Inglis, Phys. Rev. **50**, 783 (1936).

METHOD

Equations (1) and (2) are difficult to solve analytically. The differential analyzer at UCRL has therefore been used to study the eigenvalue problem. The machine can be programmed to generate the solutions of Eqs. (1) and (2) for an arbitrary potential plotted on the input table. The eigenvalue problem is solved by setting boundary conditions corresponding to different binding energies into the machine and generating the solutions for these energies. The eigenvalue is approximately equal to the energy for which the solution most closely satisfies the boundary condition at large r.

Three initial conditions must be set into the machine: the binding energy, the value of the wave function at some point inside the potential, and the slope at the same point. For s-states these conditions were set at $r=0$ so that no approximations were involved. For higher angular momentum states the potential curves

cannot be plotted to $r=0$ since the centifugal and the spin-orbit potentials are singular at the origin. It has been assumed, therefore, that for small values of $r(r \leqslant b)$ the solutions of the equation are spherical Bessel functions (that is, the potential near the origin is a square well of depth V_{0n}). The slope and value of the Bessel function were calculated[8] at $r=b$ and set into the machine, which then solved the differential equation for $r>b$. The radius, b, is chosen as small as possible in order to minimize the error involved in this procedure (b ranges from 2×10^{-13} cm for p states to 4×10^{-13} cm for i states). The error introduced by this approximation was estimated by first-order perturbation theory and was found to be less than 0.001 Mev.

The same procedure is applied to find the energies of the proton levels except that now the initial conditions at $r=b$ are more difficult to obtain since the solutions for a square well with a uniform charge distribution are not tabulated. The initial conditions were obtained by assuming that the solution in the region $0<r \leqslant b$ is $j_l(kr)$, where k is as yet undetermined. The Coulomb potential introduces a difference, ΔE_C, in energy from the square well solution. This is estimated from first-order perturbation theory, which gives

$$\Delta E_C = N \int_0^b j_l{}^2(kr)$$

$$\times \left[-V_{0p} - E + \frac{Ze^2}{2a} \left(3 - \left(\frac{r}{a} \right)^2 \right) + \frac{\hbar^2 k^2}{2m} \right] r^2 dr, \quad (3)$$

where $\sqrt{N}$ is the normalization factor of the wave function. The number k is then chosen so that ΔE_C vanishes. For small value of kr, $j_l(kr)$ can be replaced by[9]

$$\frac{(kr)^l}{1 \cdot 3 \cdots (2l+1)},$$

and when the indicated integration is performed, the following equation for k is obtained:

$$k^2 = \frac{2m}{\hbar^2} \left\{ V_{0p} + E - \frac{3Ze^2}{2a} + \frac{Ze^2}{2a^3} b^2 \frac{(2l+3)}{(2l+5)} \right\} \quad (4)$$

$$\text{where } E < 0.$$

The remaining error is identical to that obtained in the neutron approximation and is of the order of 0.001 Mev.

The eigenvalues quoted are accurate to approximately 0.1 Mev. This error is primarily due to inherent inaccuracies in setting the initial conditions into the differential analyzer. The magnitude of this error was determined empirically. Other errors arising from improper functioning of the machine and from approxi-

mations made in the boundary conditions are small compared to this.

RESULTS

Neutrons

The top levels of various nuclei were first investigated with $\alpha = 2.02 \times 10^{+13}$ cm^{-1}, $\lambda = 30.74$, $r_0 = 1.35 \times 10^{-13}$ cm, and $V_{0n} = 39.7$ Mev. As pointed out by one of us,[10] this value of α (which corresponds roughly to a surface layer of 2.18×10^{-13} cm) is similar to one which gives the low-energy giant s-wave resonances in the neutron scattering cross section at $A = 63$ and 183. The value of λ corresponds to a spin-orbit splitting which has appeared, in the course of other calculations, to give the best over-all fit in the case of the finite square well of this radius. The well depth was chosen to give roughly the right binding energy for the $3p_{\frac{1}{2}}$ level in Pb^{208}. Since all subsequent work was carried out using a radius of $1.3A^{\frac{1}{3}} \times 10^{-13}$ cm, the results have been presented as if the radius were $1.3A^{\frac{1}{3}} \times 10^{-13}$ cm. This is easily done by noting that Eq. (1) is invariant under the transformation

$$V_0' r_0'^2 = V_0 r_0^2, \quad \lambda' V_0' = \lambda V_0, \quad \alpha' r_0' = \alpha r_0,$$
$$r_0 r' = r_0' r, \quad E_0' r_0'^2 = E_0 r_0^2, \quad (5)$$

that is, if it is desired to maintain the same level sequence, then the values α, λ, V_0, and E depend on r_0 in the above way. According to Eq. (5) the original parameters become $\alpha = 2.098 \times 10^{13}$ cm^{-1}, $\lambda = 28.51$, $V_{0n} = 42.8$ Mev under this transformation. The results for the level orderings are shown in Fig. 1.

It may be seen from Fig. 1 that the situation is considerably improved from that in the square well. In order to demonstrate the shift of the levels as a function of the potential slope alone the square wells have the same depth as the diffuse potential, V_{0n}. This value is somewhat deeper than the one which would give the proper binding energy of the top level in the square well. A shell is now obtained at $N = 126$ and the one at $N = 82$ is improved. The states of higher angular momentum have been raised relative to those of lower angular momentum as demonstrated, for example, by the fact that the $1i_{13/2}$ level is now less bound than the $2f_{7/2}$ level. However, the high angular momentum states are still too low. From single-particle assignments deduced from experimentally observed ground-state spins and parities,[11] the last level in the $N = 20$ shell should be $1d_{3/2}$ rather than $2s_{1/2}$. The first level appearing beyond $N = 28$ should be $2p_{3/2}$, not $1f_{5/2}$, and the first level beyond $N = 50$ should be $2d_{5/2}$, not $1g_{7/2}$. The last level before $N = 82$ should be $2d_{3/2}$, not $3s_{1/2}$; and the first level after $N = 82$ should be $2f_{7/2}$, not $1h_{9/2}$.

In order to see whether the experimental level sequence could be obtained, both α and λ were varied.

[8] *Tables of Spherical Bessel Functions*, National Bureau of Standards (Columbia University Press, New York, 1947).

[9] See for example, L. I. Schiff, *Quantum Mechanics* (McGraw-Hill Book Company, Inc., New York, 1955), second edition, p. 78.

[10] R. D. Lawson, Phys. Rev. **101**, 311 (1956).

[11] M. G. Mayer and J. H. D. Jensen, reference 2, pp. 74–81.

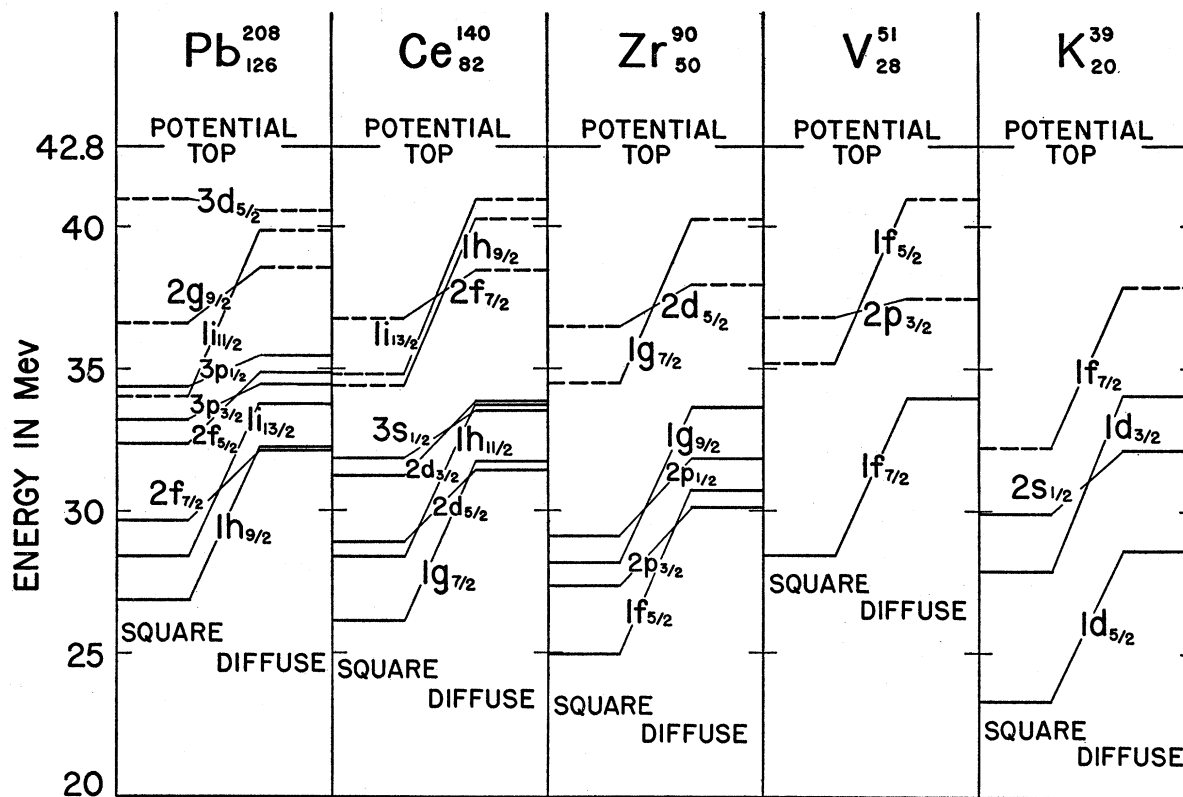FIG. 1. Top neutron levels in nuclei with $N=20$, 50, 82, and 126. The diffuse well levels have been calculated for $V_0=42.8$ Mev, $\lambda=28.51$, $\alpha=2.098\times10^{13}$ cm^{-1}, and $r_0=1.3\times10^{-13}$ cm. The square well levels have been determined for the same V_0, λ, and r_0. The level shifts shown in this figure are less pronounced than those obtained with the smaller value of α in Fig. 4. The dotted lines indicate unfilled levels. Notice that the unfilled $1i_{11/2}$ level in Pb^{208} is actually below the top $(3p_{1/2})$ neutron level in the square well, a defect which is corrected by sloping the potential.

Some idea of the manner in which different states shift with varying surface layer, Δ, may be obtained from Fig. 2. First-order perturbations calculations, which treat the sloping of the side as a perturbation from the square well (but do not take into account the diffusity of the spin-orbit term), are inadequate to estimate the positions of the levels. The magnitude of the error depends on the angular momentum, the thickness of the surface layer and on the binding energy in question. For example, in Ce^{140} with $\alpha=2.098\times10^{13}$ cm^{-1}, $\lambda=28.51$, $r_0=1.3\times10^{-13}$ cm, and $V_0=42.8$ Mev perturbation theory underestimated the shift of the $2f_{7/2}$ level by 40%, the $1h_{9/2}$ by about 9% and the $2d_{5/2}$ by about 12%. For small α (large surface layer, Δ,) perturbation theory overestimates the shift. Both effects may be understood by noting that the diffuse-well eigenfunctions (some examples of which are given in Fig. 3) tend to extend out further than those in the square well. Thus for large α the state tends to be bound more loosely than the perturbation estimate, since the wave function increases more in the interior region than the exterior region. On the other hand, for small α the state is more tightly bound, since the

increase of the wave function in the exterior region becomes more important.

The possible changes in α and λ can be seen by bearing in mind that an increase in surface layer raises levels by an amount roughly proportional to the orbital angular momentum.[12] On the other hand, increasing the spin-orbit coupling will shift levels by amounts again roughly proportional to the orbital angular momentum but will lower levels with $j=l+\frac{1}{2}$ and raise levels with $j=l-\frac{1}{2}$. It should also be remembered that the magnitude of the spin-orbit splitting for a level of given orbital angular momentum l depends not only on l and the number of nodes, but also, as in the square well, upon the binding energy of the level, and decreases as the binding becomes tighter. Thus a knowledge of the separation and even the sequence of a group of tightly bound levels gives no more than a crude idea of their behavior when they are the top levels in a nucleus. A comparison of the neutron levels shown in

[12] It is interesting to note that the binding energy is not always decreased for increasing surface layer since a sufficiently lightly bound state feels an increase in binding energy because a large proportion of its wave function lies outside the nuclear radius. The $3d_{5/2}$ level in Pb^{208} in Fig. 4 is an example of this.

Fig. 4 with those for neutrons in Au[197] shown in Fig. 5 illustrates this point clearly.

In the square well the "center of gravity" of two levels with the same orbital angular momentum, l, and different total angular momentum, j, shifts downwards as the spin-orbit coupling is increased. For example, in Ce[140], for $r_0 = 1.3 \times 10^{-13}$ cm, $V_0 = 42.8$ Mev, and $\lambda = 28.51$, the splitting of the h-states is 4.24 Mev and the center of gravity of the split levels has descended 0.48 Mev from its position when $\lambda = 0$. If $\lambda = 39.5$, the splitting is proportionally increased to 5.96 Mev and the center of gravity has now descended an additional 0.43 Mev. However, in the diffuse well with the same parameters, except that $\Delta = 2.1$, the splitting of the h-states is 4.70 for $\lambda = 28.51$, and for $\lambda = 39.5$ the splitting is proportionally 6.5 Mev but the center of gravity is now shifted down only by an additional 0.01 Mev. This means that in a diffuse well (for $\Delta \approx 2-3 \times 10^{-13}$ cm) it is easy to estimate the effect of changing λ when one set of solutions is known. However, since the square-well center of gravity descends, it also implies

that curves such as those shown in Fig. 2 will be different for two different λ's.

Although the absolute shift in a level is not linear in Δ, in the interesting region of Δ it is as good and much quicker to estimate the relative shifts of neighboring levels on a linear basis, rather than to perform a perturbation calculation. This is especially true if the levels also have angular momenta which are close. Actually the curves showing the shift of levels as the surface layer is increased show the following general form: the derivative is zero at $\Delta = 0$, the curve becomes gently concave upwards, then passes through a turning point and gradually flattens off. In addition, for smaller binding energies, lower angular momenta, or larger number of nodes, the flat region is reached sooner. Making rough allowances for this, it is not difficult to make a reasonably good guess of relative level shifts when solutions are known for some value of α and λ in the region of interest.

If one requires that in Ce[140] the $2d_{3/2}$ level be the last bound state and that the $1h_{11/2}$ level lie between it and the $3s_{1/2}$, at the same time keeping λ as small as possible, then there is little choice but to take values close to $\alpha = 1.45 \times 10^{13}$ ($\Delta \approx 3 \times 10^{-13}$ cm) and $\lambda = 39.5$. The results with these parameters and $V_0 = 42.8$ Mev are shown in Fig. 4. It is noticeable that all the desired crossovers of levels have now occurred. In fact, the only region which now does not exhibit close agreement with level sequences deduced from single-particle assignments is the middle of the $N = 82-126$ shell. This might be
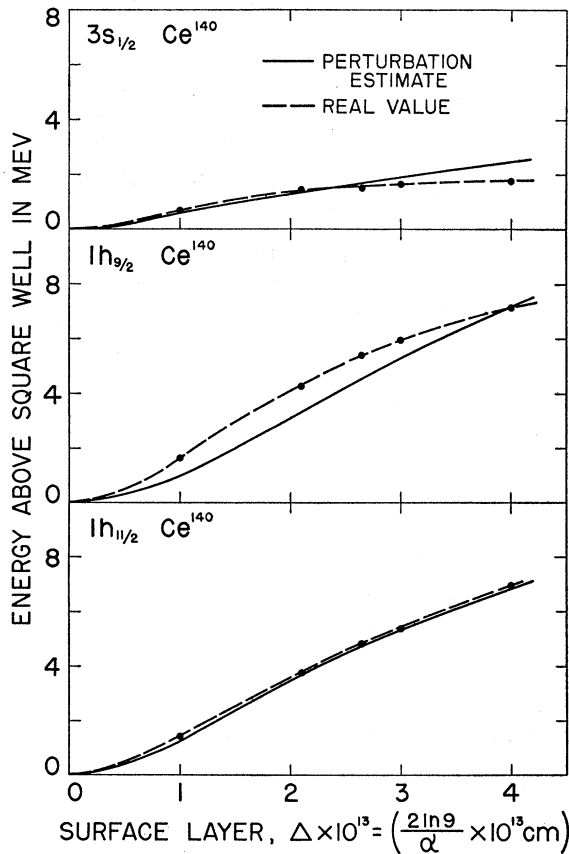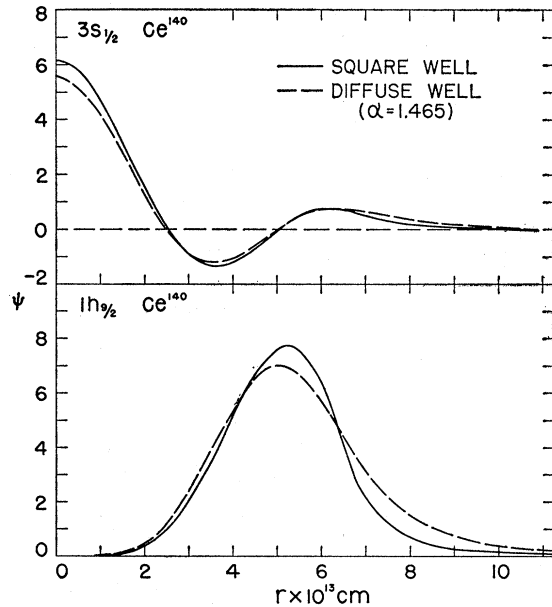

FIG. 2. The energy shift of three representative levels as the surface layer of the potential is increased. The solid curves show the shifts estimated from first-order perturbation theory, and the dotted lines show the actual level shifts obtained with the differential analyzer.

FIG. 3. Wave functions for a diffuse ($\alpha = 1.465 \times 10^{13}$ cm^{-1}) and square potential for the $3s_{1/2}$ and the $1h_{9/2}$ states in Ce[140]. In each case, the wave function in the diffuse potential has a larger amplitude outside the nucleus. The diffuse-potential wave functions were taken directly from curves generated by the differential analyzer.
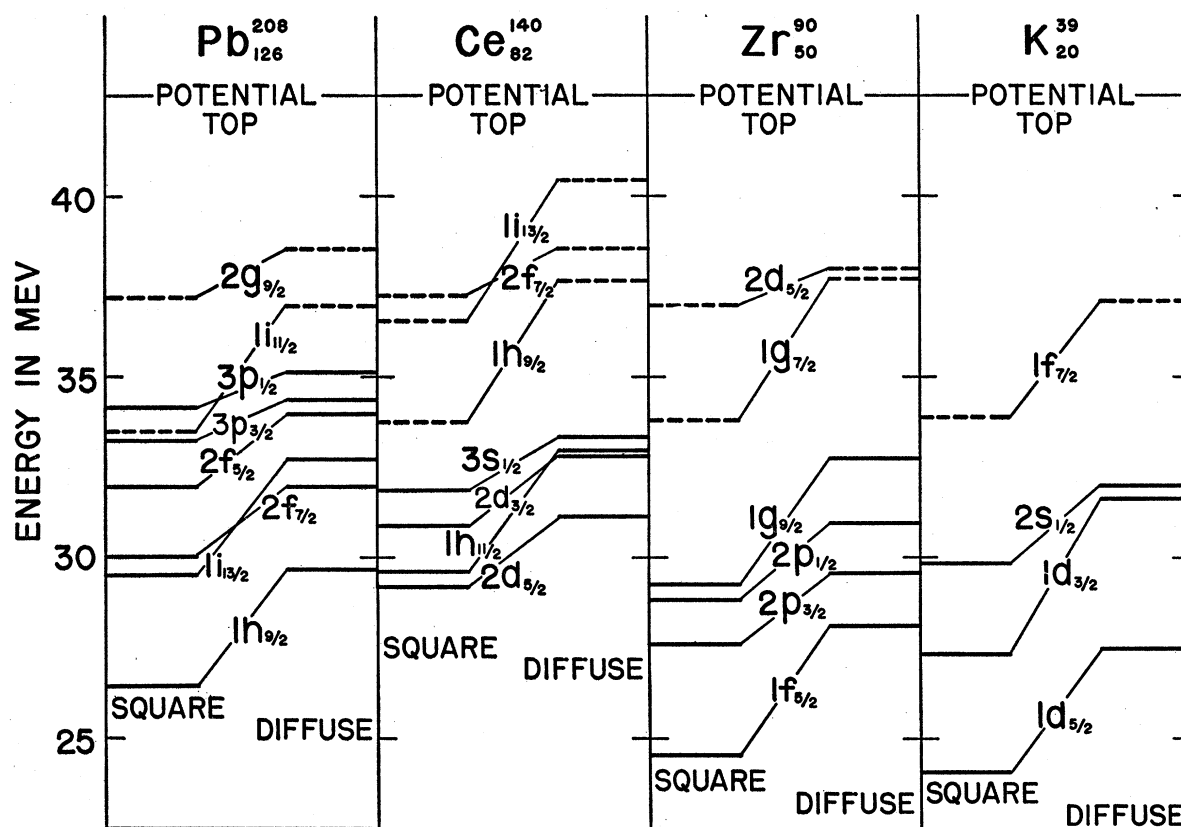
FIG. 4. Top neutron levels with $N=20$, 28, 50, 82, and 126. The diffuse well levels have been calculated for $V_0=42.8$ Mev, $\lambda=39.5$, $\alpha=1.45\times10^{13}$ cm^{-1}, and $r_0=1.3\times10^{-13}$ cm. The dotted lines indicate unfilled levels.

expected, since it is the region of strong distortion[13] where a spherically symmetric potential should bear little resemblance to reality.

The requirement that the $1h_{11/2}$ level lie between the $2d_{3/2}$ and $3s_{1/2}$ levels is possibly too stringent, since presumably two nucleons in this level have a large pairing energy. If this condition is relaxed, then either the spin-orbit coupling can be decreased somewhat or the slope can be increased without impairing the sequence elsewhere.

The well depth, V_{0n}, was chosen to be 42.8 Mev from consideration of the (γ,n) threshold[14] in Pb^{208}. Since the top state in this nucleus is a low-l state, $3p_{1/2}$, presumably the pairing energy is small.[15] The binding energy of the $2d_{3/2}$ particle in Ce^{140} is then approximately 8.95 Mev, in agreement with the experimental value of (9.05 ± 0.2) Mev. For the lighter elements, the calculated binding energies are smaller than the (γ,n) thresholds. However, in Zr^{90} the top state is $1g_{9/2}$ and in V^{51} the

top neutron is in a $1f_{7/2}$ level, so that perhaps pairing energy becomes more important. However, if pairing energy is neglected, then the potential well depth for neutrons increases for light nuclei. This would improve the spacing of the $2p_{3/2}$ and $1f_{5/2}$ levels in V^{51} by bringing them closer together, since both would then experience less spin-orbit splitting because of their tighter binding.

For $\alpha=1.45\times10^{13}$ cm^{-1}, $r_0=1.3\times10^{-13}$ cm, and $V_0=42.8$ Mev, the 3s and 4s giant resonances in the low-energy neutron scattering cross section occur at $A=56$ and $A=166$, respectively, in good accord with experiment.[16] If α is further decreased, these resonances will occur for smaller A.

Protons

For protons it was assumed that α, λ, and r_0 had the same values and in addition that the Coulomb repulsion was derivable from a uniform charge distribution extending out to the nuclear radius, a. The required well depths are, however, somewhat larger than for neutrons. Since the (γ,p) thresholds are somewhat more uncertain than the (γ,n) thresholds, the values

[13] A. Bohr and B. R. Mottelson, Kgl. Danske Videnskab. Selskab, Mat.-fys. Medd. **27**, No. 16 (1953).

[14] See for example, Sher, Halpern, and Mann, Phys. Rev. **84**, 387 (1951), and the references quoted in their paper.

[15] One can perhaps get some idea of the magnitude of the pairing energy in this state by comparing the (γ,n) threshold in Pb^{207} and Pb^{208}. The threshold in Pb^{208} is approximately 0.6 Mev greater than in Pb^{207}, so that one might argue that the well depth chosen was approximately 0.6 Mev too deep.

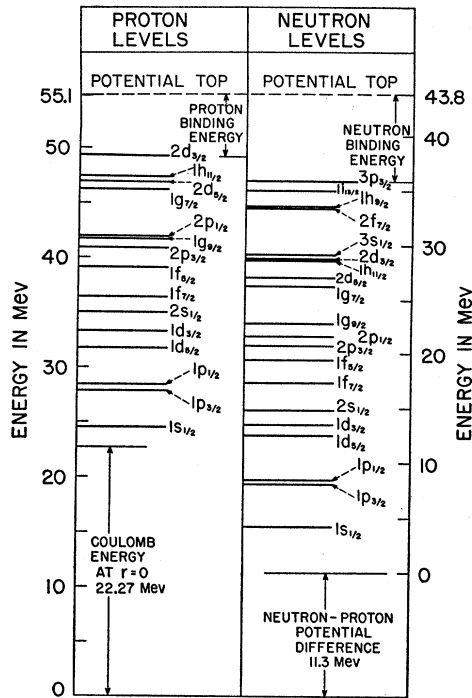[16] Feshbach, Porter, and Weisskopf, Phys. Rev. **90**, 166 (1953), and **96**, 448 (1954).

FIG. 5. Proton and neutron levels in Au[197]. The proton levels have been calculated assuming a uniform charge distribution out to the nuclear radius. The values of λ, α, and r_0 used are the same for both wells ($\lambda=39.5$, $\alpha=1.45\times10^{13}$ cm^{-1}, and $r_0=1.3\times10^{-13}$ cm). The different potential well depths necessary to give the proper neutron and proton binding energies are shown in the drawing.

of V_{0p} chosen for the various nuclei are not significant. The only well depth which was chosen to agree with the (γ,p) threshold was in Pb[208] which gave a binding energy of 7.3–7.4 Mev, in agreement with the experimental results of Weinstock and Halpern.[17] The level sequences obtained are illustrated in Fig. 6. In contrast to the neutron levels, it is noticeable that the last level at the $Z=82$ shell is $3s_{1/2}$, in agreement with the assignment for the ground state of Tl[205], and that the next level is $1h_{9/2}$, in agreement with the ground state of Bi[209]. In general, close agreement is again obtained with experiment except in the middle of the $Z=50$ to $Z=82$ shell, which, for protons, is the region of large distortion.

Nucleon Densities

In order to gain some idea of the self-consistency of this potential, the density of neutrons and of protons was calculated assuming

$$\rho_p(r)= \sum_{\text{protons}} |\psi_p(r)|^2, \quad \rho_n(r)= \sum_{\text{neutrons}} |\psi_n(r)|^2,$$

where $\psi_{p,n}$ is the shell-model wave function neglecting interparticle interactions, and assuming that all nucleons in the nucleus move in the same potential. In view of the recent electron scattering experiments, it was felt that it would be interesting to examine the charge distribution obtained for Au[197], the case for which the most theoretical work has been carried out. The neutron potential depth was chosen to be 43.8 Mev, which yields a binding energy of 7.9–8 Mev for the top
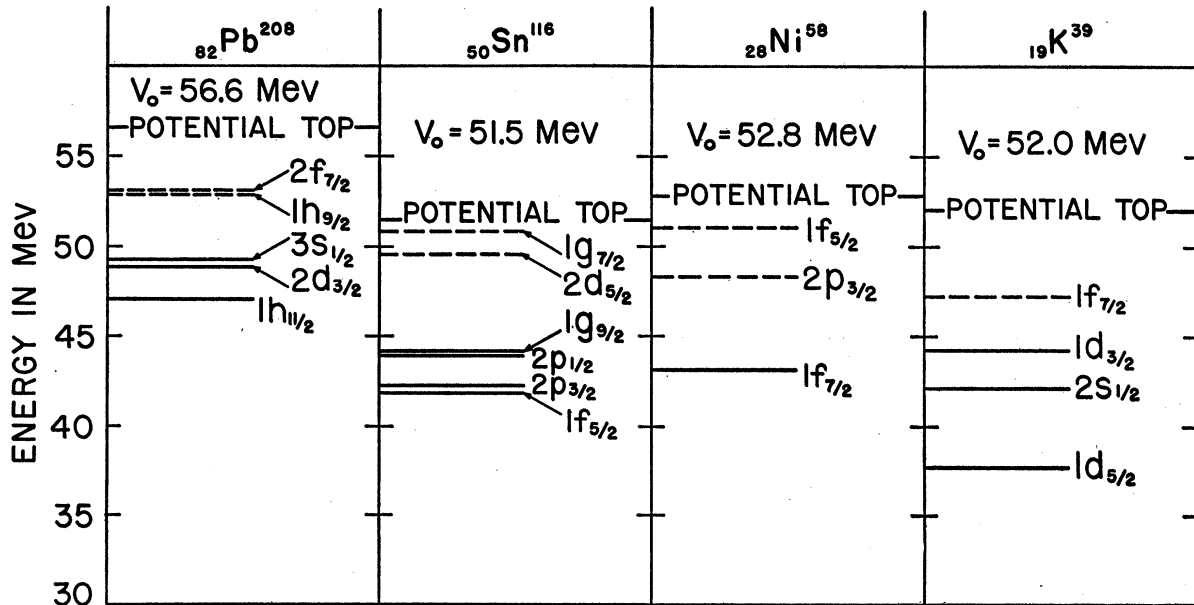

FIG. 6. Top proton levels in nuclei with $Z=19$, 28, 50, and 82. The ordering of the top three levels in Pb[208] ($Z=82$) is changed from the ordering of the top three neutron levels in Ce[140] ($N=82$) (see Fig. 4). The low angular momentum levels ($3s_{1/2}$ and $2d_{3/2}$) are raised with respect to the $1h_{11/2}$ level because of the additional Coulomb potential.

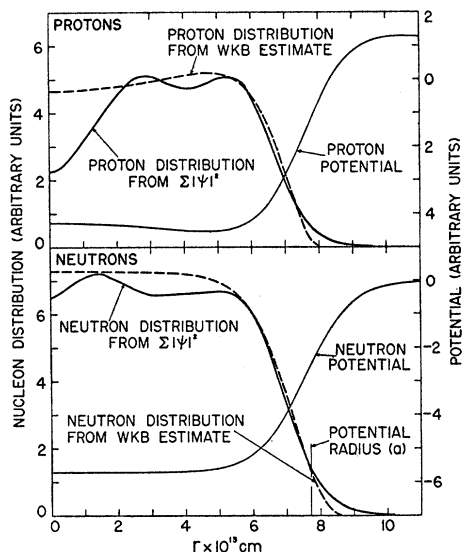[17] E. V. Weinstock and J. Halpern, Phys. Rev. 94, 1651 (1954).

FIG. 7. Proton and neutron density distributions in Au[197] obtained by the WKB approximation and by actually summing the squares of all particle wave functions. The potentials used to compute these distributions are also displayed.

neutron, in agreement with work of Nathans and Halpern.[18] For protons the depth was taken as 55.1 Mev, which implies the last proton is bound by 5.8 Mev, in agreement with Weinstock and Halpern.[17]

The proton and neutron densities are shown in Fig. 7. The proton distribution as derived from $\sum_{\text{protons}} |\psi_p|^2$ has a decided hole at $r=0$. This effect is due to at least two causes: first, the Coulomb repulsion at the center of the nucleus tends to push particles away from $r=0$; second, for the gold nucleus, the $3s_{1/2}$ state is not yet bound. Since only the s-state wave functions have a value different from zero at $r=0$, this will cause a dip in the distribution. The proton and neutron surface layers, defined in the usual way in terms of the edge peak value, are 1.92×10^{-13} cm and 2.20×10^{-13} cm, respectively. The radius of the proton distribution is 6.77×10^{-13} cm (corresponding to an r_0 of $[6.77/(197)^{\frac{1}{3}}]$ $\times 10^{-13} = 1.16 \times 10^{-13}$ cm), and for the neutron distribution, 6.98×10^{-13} cm $(r_0 = 1.2 \times 10^{-13}$ cm). According to the latest Stanford calculations[5] the electron-scattering results can be best explained by a proton distribution which has a dip in the center (although not as pronounced as the one found here), a radius of (1.07 ± 0.2)

$\times 10^{-13}$ $A^{\frac{1}{3}}$ cm and a surface layer of approximately 2.4×10^{-13} cm. It therefore appears that the radius we have chosen for our potential, $1.3 \times 10^{-13} \times A^{\frac{1}{3}}$, is too large to give a change distribution in agreement with experiment and should be decreased by approximately 8%. The radius of the Coulomb potential should also be taken, for greater consistency, as less than the radius of the potential. On the other hand, the surface layer on the charge distribution is too small and consequently a smaller value of α must be chosen $(\alpha \approx 1 \times 10^{13}$ cm$^{-1})$ to agree with electron-scattering results. Although the differential equation describing the proton, Eq. (2), does not have the same invariance properties as Eq. (1), the effect of changing r_0 will be to modify only slightly the energy level sequence and thus the density.

The fact that the neutron distribution lies outside the proton distribution is in agreement with the prediction of Johnson and Teller.[19] The effect, however, is somewhat smaller than they estimated, for two reasons: first, the last proton in gold is bound approximately 2 Mev less tightly than the last neutron, whereas in Johnson and Teller's estimate the neutron and proton had the same binding energy; second, their nuclear potential was assumed to be the same for neutrons and protons, whereas in this work the proton potential is considerably deeper. However, the neutron distribution does have a considerably longer tail than the proton distribution. This is because the neutron wave functions are not damped out by the Coulomb barrier.

The proton and neutron distributions have also been calculated using the WKB approximation (also shown in Fig. 7). For protons the radius is 6.87×10^{-13} cm and the surface layer is 1.71×10^{-13} cm, whereas for neutrons the radius is 6.98×10^{-13} cm and the surface layer 2.38×10^{-13} cm. Both these results are in reasonable agreement with the exact calculation, so that the qualitative features at least of the surface region can be obtained from WKB approximation. The neutron and proton potential have also been plotted on the same diagram to show the relationship between the nucleon density and the potential. It will be noted that the nucleon density follows reasonably well the form of the potential.

ACKNOWLEDGMENTS

[18] R. Nathans and J. Halpern, Phys. Rev. 93, 437 (1954).

[19] M. H. Johnson and E. Teller, Phys. Rev. 93, 357 (1954).